YMTHE, Volume *29*

Supplemental Information

Enforced dimerization between XBP1s and ATF6f enhances the protective effects of the UPR in models of neurodegeneration

René L. Vidal, Denisse Sepulveda, Paulina Troncoso-Escudero, Paula Garcia-Huerta, Constanza Gonzalez, Lars Plate, Carolina Jerez, José Canovas, Claudia A. Rivera, Valentina Castillo, Marisol Cisternas, Sirley Leal, Alexis Martinez, Julia Grandjean, Donzelli Sonia, Hilal A. Lashuel, Alberto J.M. Martin, Veronica Latapiat, Soledad Matus, S. Pablo Sardi, R. Luke Wiseman, and Claudio Hetz

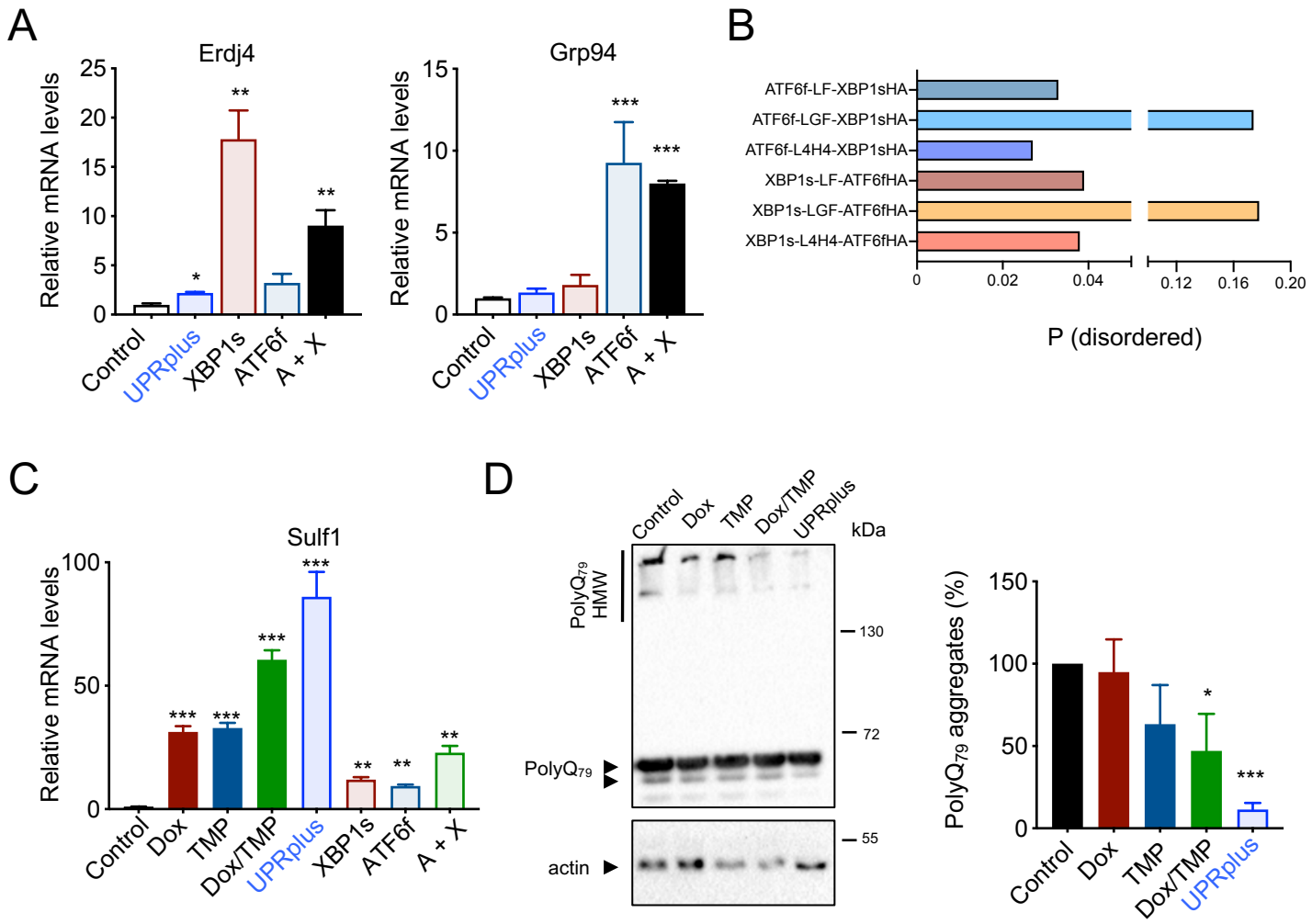
A
Erdj4
Grp94
Relative mRNA levels
Control
UPRplus
XBP1s
ATF6f
A + X
B
ATF6f-LF-XBP1sHA
ATF6f-LGF-XBP1sHA
ATF6f-L4H4-XBP1sHA
XBP1s-LF-ATF6fHA
XBP1s-LGF-ATF6fHA
XBP1s-L4H4-ATF6fHA
P (disordered)
C
Sulf1
Dox
TMP
Dox/TMP
D
kDa
PolyQ79 HMW
PolyQ79
actin
130
72
55
PolyQ79 aggregates (%)

Figure S1

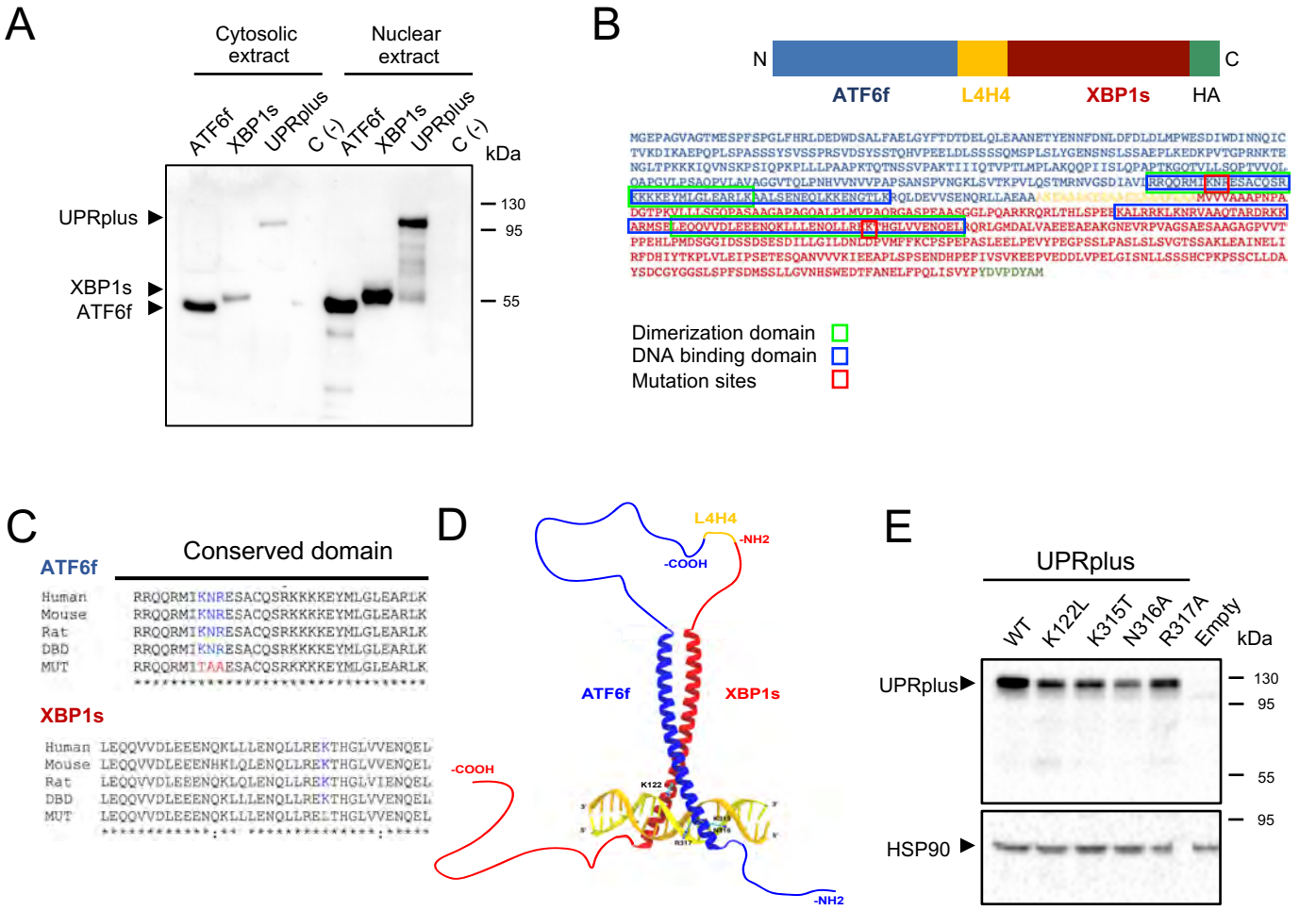
A
Cytosolic extract
Nuclear extract
ATF6f
XBP1s
UPRplus
C (-)
ATF6f
XBP1s
UPRplus
C (-)
kDa
UPRplus
XBP1s
ATF6f
130
95
55
B
N
C
ATF6f
L4H4
XBP1s
HA
Dimerization domain
DNA binding domain
Mutation sites
C
Conserved domain
ATF6f
Human RRQQRMIKNRESACQSRKKKKEYMLGLEARLK
Mouse RRQQRMIKNRESACQSRKKKKEYMLGLEARLK
Rat RRQQRMIKNRESACQSRKKKKEYMLGLEARLK
DBD RRQQRMIKNRESACQSRKKKKEYMLGLEARLK
MUT RRQQRMITAAESACQSRKKKKEYMLGLEARLK
XBP1s
Human LEQQVVDLEEENQKLLLENQLLREKTHGLVVENQEL
Mouse LEQQVVDLEEENHKLQLENQLLREKTHGLVVENQEL
Rat LEQQVVDLEEENQKLQLENQLLREKTHGLVIENQEL
DBD LEQQVVDLEEENQKLLLENQLLREKTHGLVVENQEL
MUT LEQQVVDLEEENQKLLLENQLLRELTHGLVVENQEL
D
L4H4
-NH2
-COOH
ATF6f
XBP1s
-COOH
K122
-NH2
E
UPRplus
WT
K122L
K315T
N316A
R317A
Empty
kDa
UPRplus
130
95
55
HSP90
95
F
UPRplus WT
UPRplus K122L
UPRplus K315T
UPRplus N316A
UPRplus R317A
HA
HA/
DAPI

Figure S2

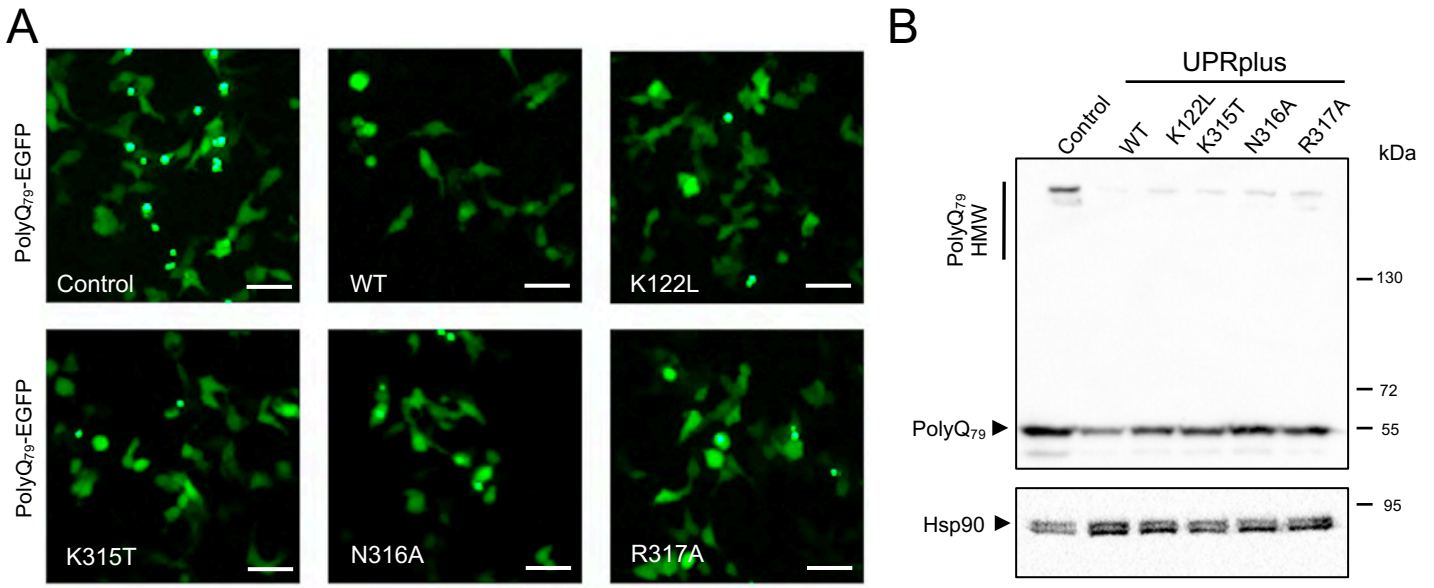
A
PolyQ79-EGFP
Control
WT
K122L
PolyQ79-EGFP
K315T
N316A
R317A
B
UPRplus
Control
WT
K122L
K315T
N316A
R317A
kDa
PolyQ79 HMW
130
72
PolyQ79
55
Hsp90
95

Figure S3

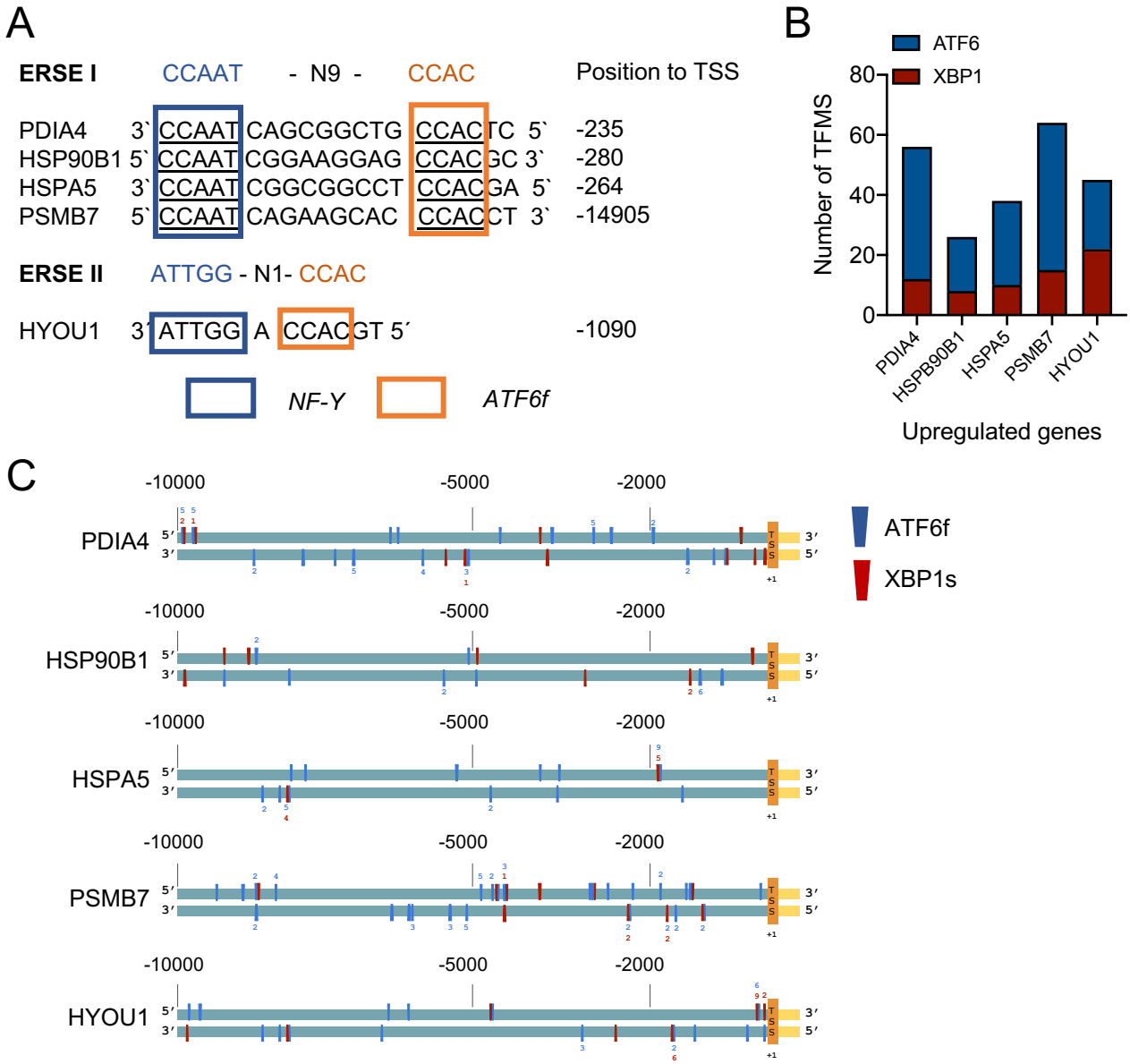
A
ERSE I
CCAAT - N9 - CCAC
Position to TSS
PDIA4 3` CCAAT CAGCGGCTG CCACTC 5` -235
HSP90B1 5` CCAAT CGGAAGGAG CCACGC 3` -280
HSPA5 3` CCAAT CGGCGGCCT CCACGA 5` -264
PSMB7 5` CCAAT CAGAAGCAC CCACCT 3` -14905
ERSE II
ATTGG - N1- CCAC
HYOU1 3´ ATTGG A CCACGT 5´ -1090
NF-Y
ATF6f
B
ATF6
XBP1
Number of TFMS
80
60
40
20
0
PDIA4
HSPB90B1
HSPA5
PSMB7
HYOU1
Upregulated genes
C
-10000
-5000
-2000
PDIA4
HSP90B1
HSPA5
PSMB7
HYOU1
ATF6f
XBP1s
D
ATF6f
XBP1s
XBP1s
ATF6f
bits

Figure S4

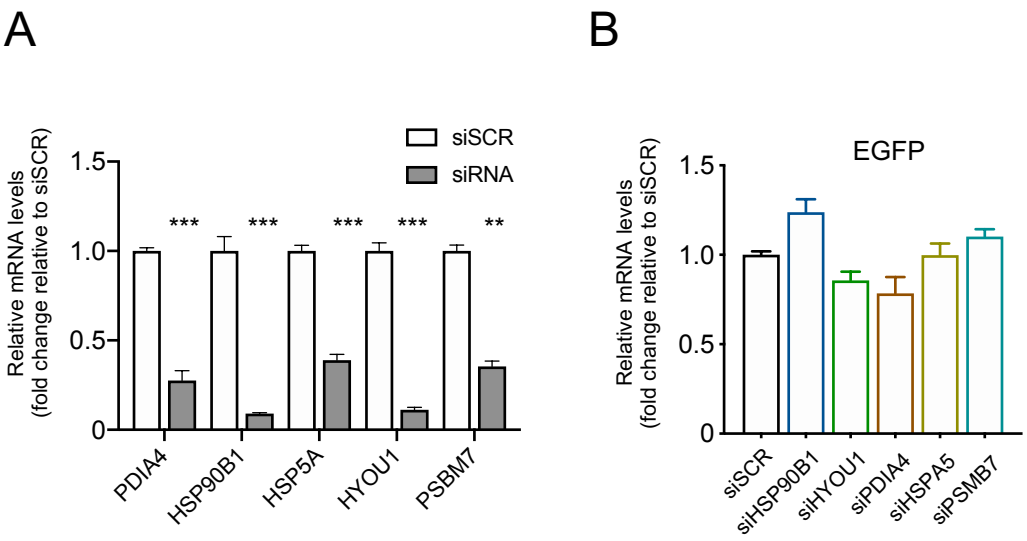
A
B
siSCR
siRNA
Relative mRNA levels
(fold change relative to siSCR)
1.5
1.0
0.5
0
***
***
***
***
**
PDIA4
HSP90B1
HSP5A
HYOU1
PSBM7
EGFP
siSCR
siHSP90B1
siHYOU1
siPDIA4
siHSPA5
siPSMB7

Figure S5

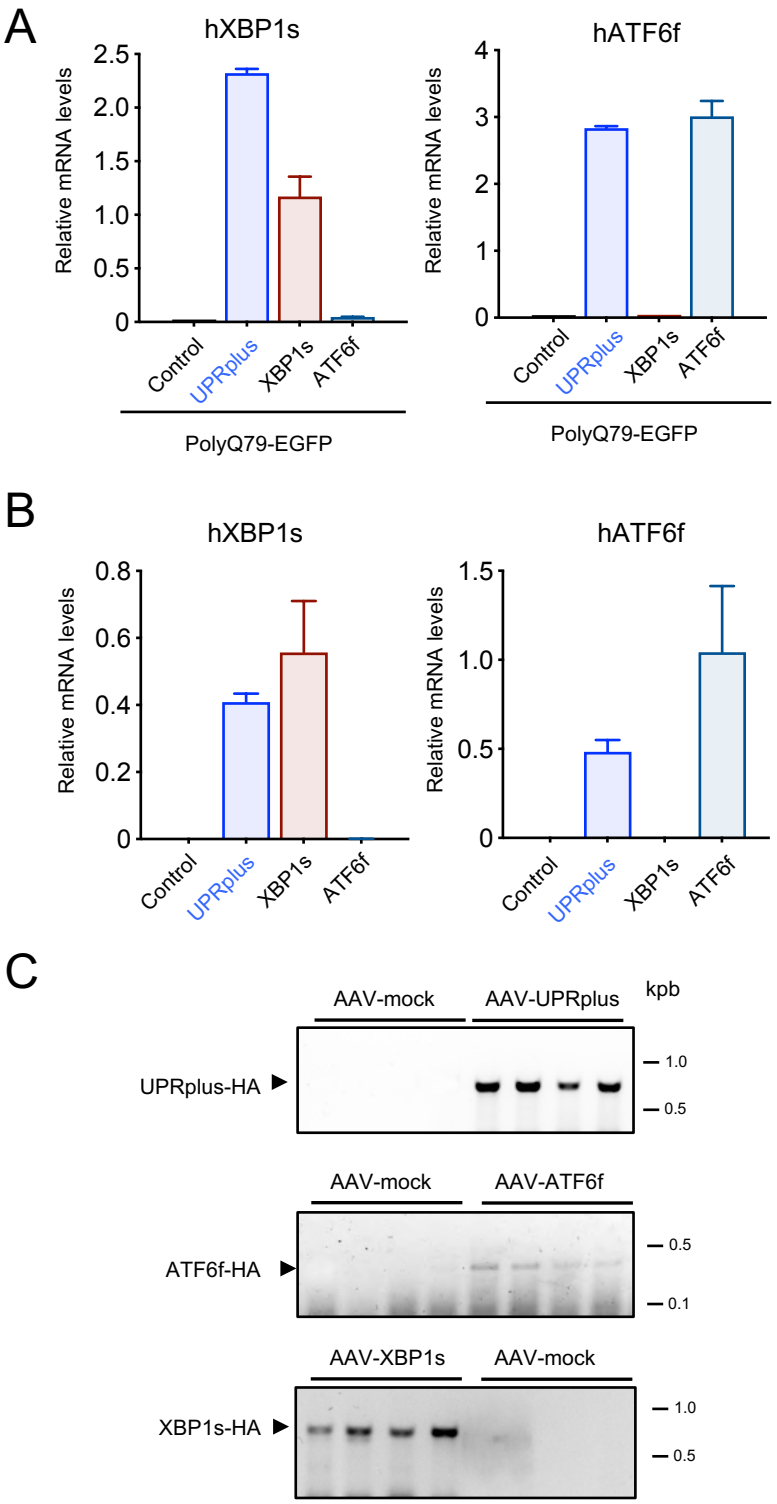
A
hXBP1s
Relative mRNA levels
2.5
2.0
1.5
1.0
0.5
0
Control
UPRplus
XBP1s
ATF6f
PolyQ79-EGFP
hATF6f
Relative mRNA levels
4
3
2
1
0
Control
UPRplus
XBP1s
ATF6f
PolyQ79-EGFP
B
hXBP1s
Relative mRNA levels
0.8
0.6
0.4
0.2
0
Control
UPRplus
XBP1s
ATF6f
hATF6f
Relative mRNA levels
1.5
1.0
0.5
0
Control
UPRplus
XBP1s
ATF6f
C
AAV-mock
AAV-UPRplus
kpb
UPRplus-HA
1.0
0.5
AAV-mock
AAV-ATF6f
ATF6f-HA
0.5
0.1
AAV-XBP1s
AAV-mock
XBP1s-HA
1.0
0.5

Figure S6

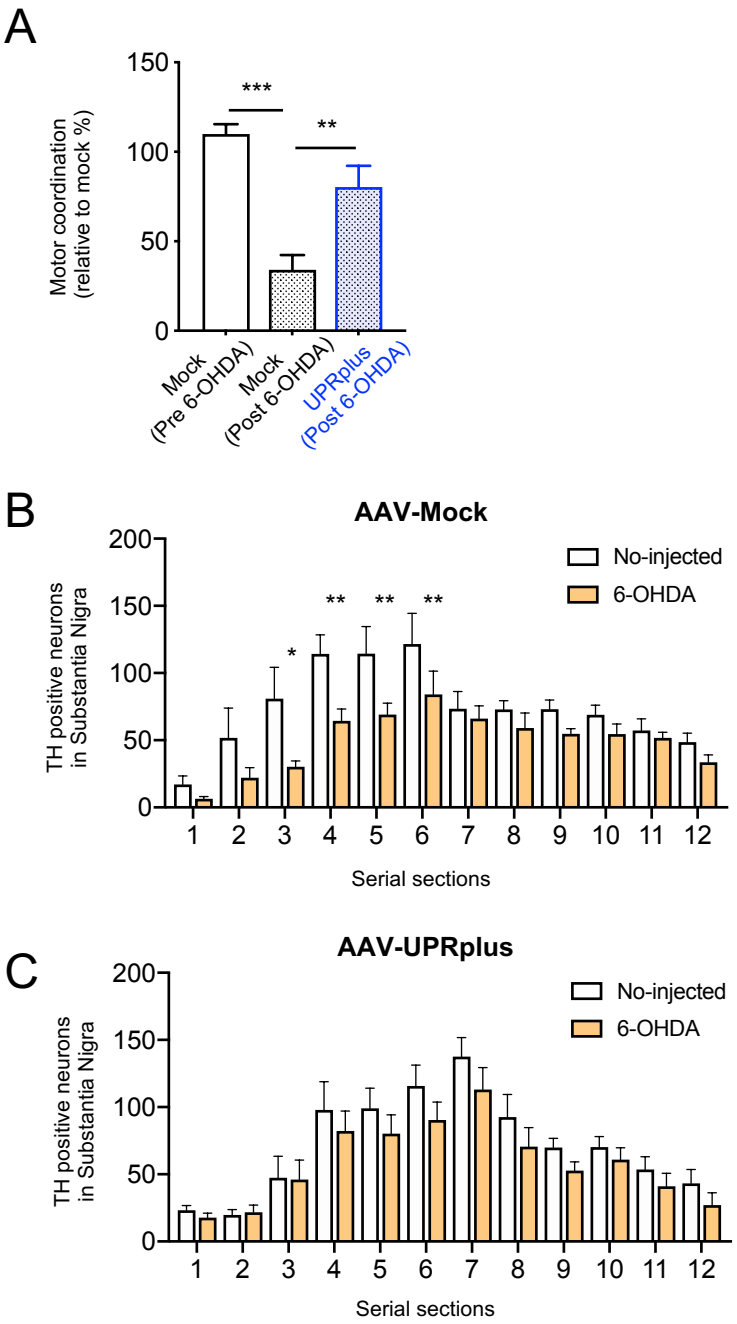
A
Motor coordination (relative to mock %)
150
100
50
0
***
**
Mock (Pre 6-OHDA)
Mock (Post 6-OHDA)
UPRplus (Post 6-OHDA)
B
AAV-Mock
No-injected
6-OHDA
TH positive neurons in Substantia Nigra
200
150
100
50
0
*
**
**
**
1 2 3 4 5 6 7 8 9 10 11 12
Serial sections
C
AAV-UPRplus
No-injected
6-OHDA
TH positive neurons in Substantia Nigra
200
150
100
50
0
1 2 3 4 5 6 7 8 9 10 11 12
Serial sections

Figure S7

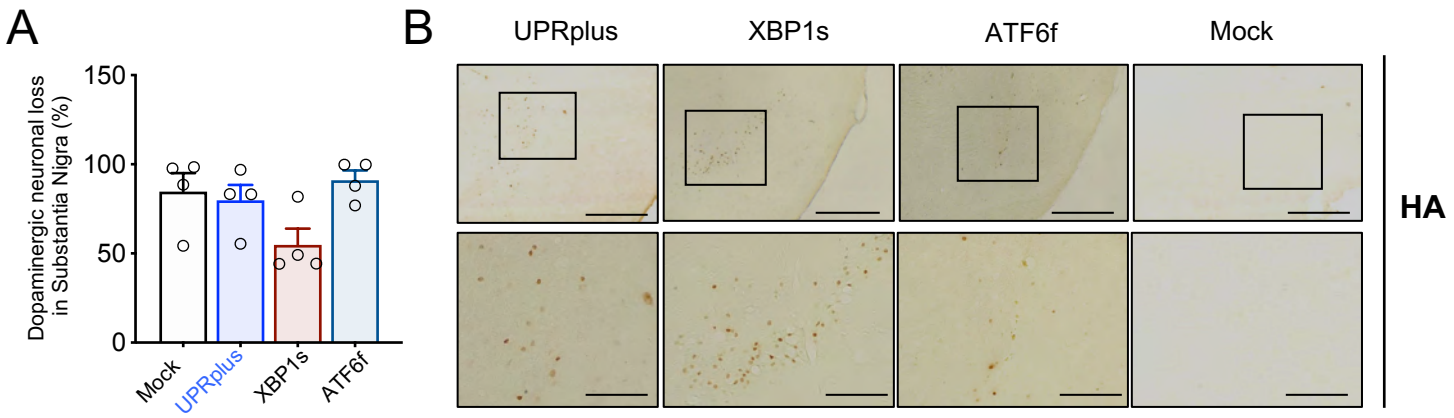
A
Dopaminergic neuronal loss in Substantia Nigra (%)
150
100
50
0
Mock
UPRplus
XBP1s
ATF6f
B
UPRplus
XBP1s
ATF6f
Mock
HA

Figure S8

A

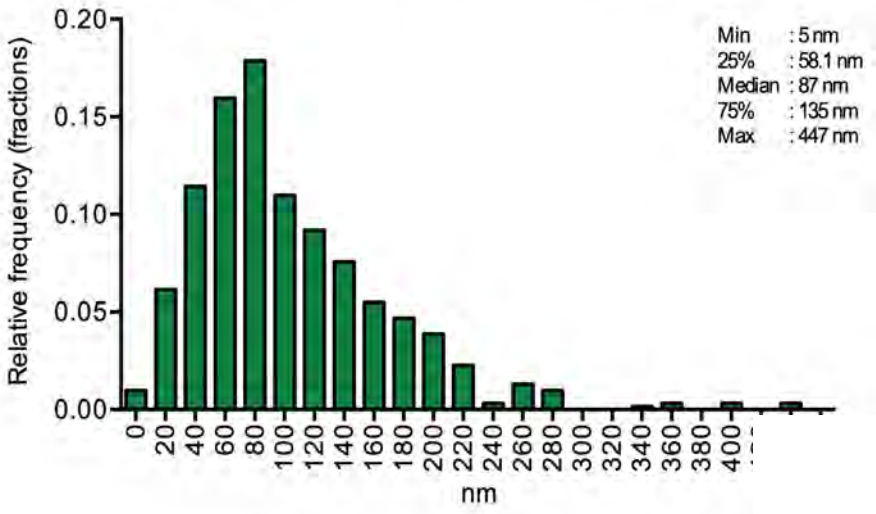
Relative frequency (fractions)
0.20
0.15
0.10
0.05
0.00
0
20
40
60
80
100
120
140
160
180
200
220
240
260
280
300
320
340
360
380
400
nm
Min : 5 nm
25% : 58.1 nm
Median : 87 nm
75% : 135 nm
Max : 447 nm

B

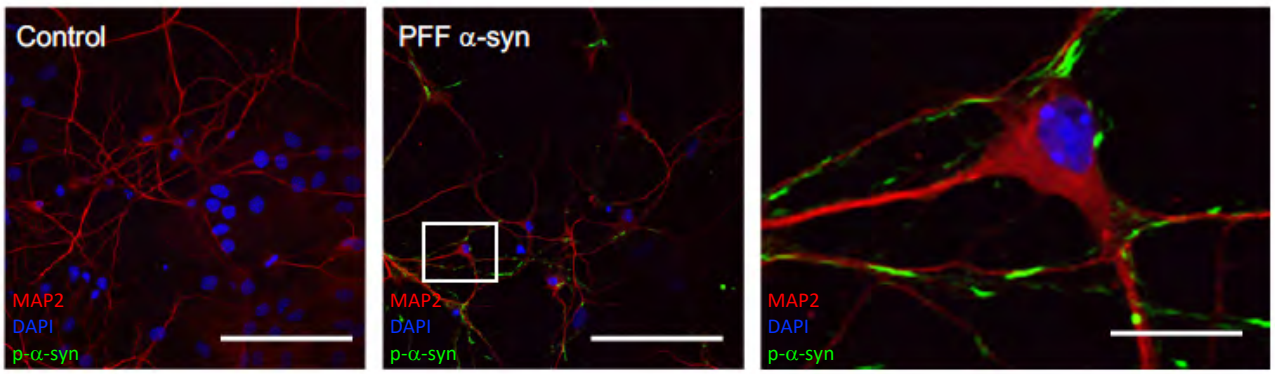
Control
MAP2
DAPI
p-α-syn
PFF α-syn
MAP2
DAPI
p-α-syn
MAP2
DAPI
p-α-syn

Figure S9

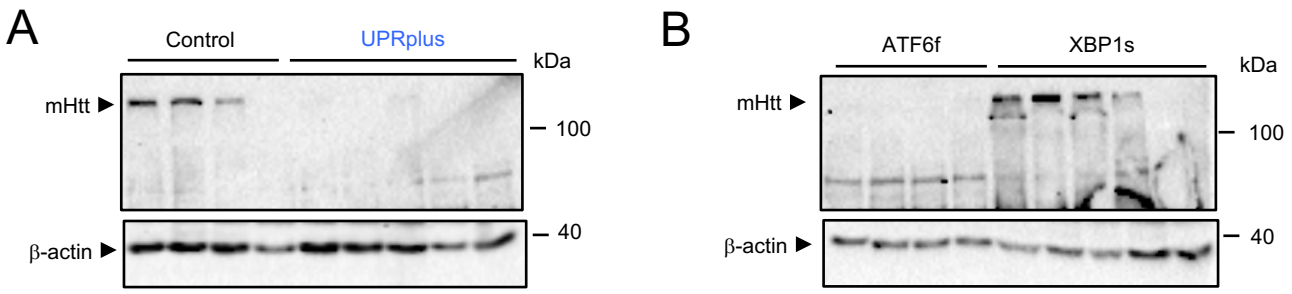
A
Control
UPRplus
kDa
mHtt
100
β-actin
40
B
ATF6f
XBP1s
kDa
mHtt
100
β-actin
40

Figure S10

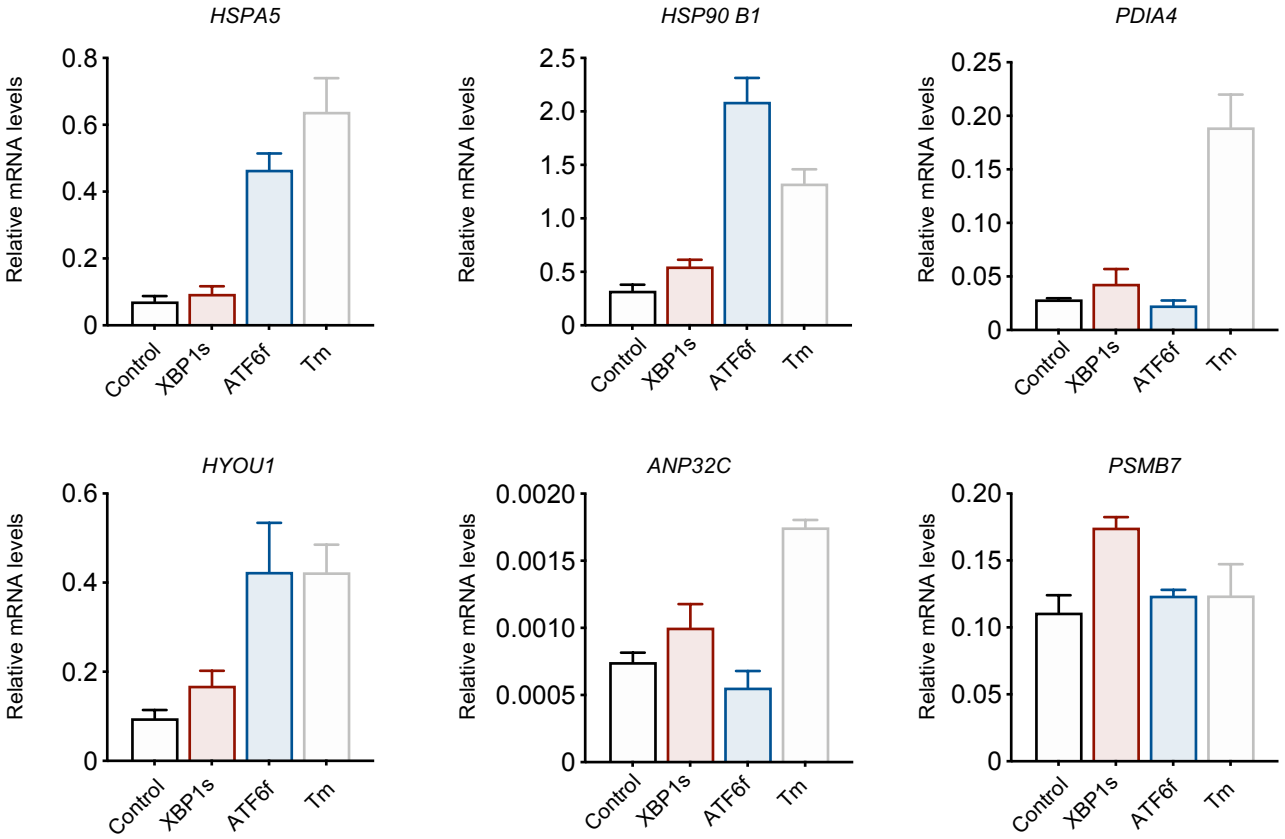
HSPA5
HSP90 B1
PDIA4
HYOU1
ANP32C
PSMB7
Relative mRNA levels
Control
XBP1s
ATF6f
Tm

Figure S11

Supplementary figure legends

Table S1. Protein expression changes triggered by the expression of UPRplus, XBP1s, and ATF6f in HEK293T cells. Quantitative proteomics was performed in protein extracts from HEK293T cells infected for 48 h with the following viral particles: AAV-UPRplus, AAV-XBP1s, AAV-ATF6f, or AAV-empty (vehicle). Fold change, q-value and Standard Deviation (SD) of 124 differential protein expression in each condition are showed. Color from red to blue indicates high to low expression.

Table S2. Protein expression changes triggered by the expression of UPRplus, XBP1s, and ATF6f in HEK293T cells. Quantitative proteomics was performed in protein extracts from HEK293T cells infected for 48 h with the following viral particles: AAV-UPRplus, AAV-XBP1s, AAV-ATF6f, or AAV-empty (vehicle). Raw data of differential protein expression in each condition are showed.

Figure S1. Determination of ATF6f and XBP1s transcriptional activity and flexibility of UPRplus construct. (A) The mRNA levels of ERdj4 (left panel) or GRP94 (right panel) genes were monitored in HEK293T cells infected with AAV-empty (control), AAV-UPRplus, AAV-XBP1s, AAV-ATF6f or AAV-XBP1s: AAV-ATF6f (1:1) viral particles. After 48 h the relative mRNA levels of indicated genes were measured by real-time PCR. All samples were normalized to β-*actin* levels. mRNA levels are expressed as fold increase over the value obtained in the control condition. (B) Quantification of the average disorder probability of primary protein structure considering the six fusion proteins used between ATF6f and XBP1s. The 0.1 default ESpritz threshold employed to annotate residues as disordered with a 5% False Positive Rate. (C) HEK-Rex DAX cells were treated by 16 hours with doxycycline (DOX) (1 uM), Trimethoprim (TMP) (10 uM) or both to induce the XBP1s or ATF6f respectively and transiently transfected with UPRplus, XBP1s, ATF6f or both XBP1s and ATF6f (A +X) vector. Relative mRNA levels of Sulf1 gene were measured by real-time PCR. All samples were normalized to β-*actin* levels. (D) polyQ$_{79}$-EGFP detergent-insoluble aggregates were measured in cell extracts describe in C prepared in Triton X100 by western blot (right panel). Levels of Hsp90 were measured as the loading control. Left panel: high molecular weight (HMW) polyQ$_{79}$-EGFP aggregates were quantified.

Figure S2. Expression levels and in silico structural analysis of UPRplus. (A) HEK293T cells were transiently transfected with HA-tagged expression vectors for UPRplus, ATF6f, XBP1s, or empty vector (control). After 48 h, cytosolic and nuclear

extracts were analyzed by western blot using an anti-HA antibody. (B) The amino acid sequence of UPRplus including, ATF6f (blue), linker (yellow), and XBP1s (red) sequence. The putative dimerization domains are highlighted in a black box. Mutated residues used in figure 2 are underlined in green. (C) Alignment of the putative dimerization domain sequences for ATF6f (upper panel) or XBP1s (lower panel). Asterisks represent the conserved residues and mutated residues are highlighted in red. (D) The three-dimensional model of a heterodimer of XBP1s and ATF6f attached to a DNA motif (see methods). The ATF6f chain corresponds to 306-367 residues and XBP1s chain to 70-131 residues. The XBP1s chain appears in red and the ATF6f chain is shown in blue with the residues K122, K315, N316, and R317 highlighted. The position of the linker (yellow) and the rest of the sequence are indicated using lines. (E) HEK293T cells were transiently transfected with the UPRplus WT, UPRplus K122K, UPRplus K315T, UPRplus N316A, or UPRplus R3177 constructs and after 48 h were analyzed by western blot using an anti-HA antibody (upper panel). Bottom panel: Levels of Hsp90 were monitored as a loading control. (F) HEK293T cells were transiently transfected with the UPRplus WT, UPRplus K122K, UPRplus K315T, UPRplus N316A, or UPRplus R3177 constructs and after 48 h were analyzed by immunofluorescence using an anti-HA antibody (green). Co-staining with the nuclear marker Hoechst (blue) was performed. Scale bar 20 μm.

Figure S3. The activity of UPRplus depends on the dimer interphase and DNA binding domain. (A) Higher magnification images of Neuro2A cells transiently co-transfected with expression vectors for polyQ$_{79}$-EGFP together with empty vector (control), UPRplus WT, or the UPRplus mutants K122L, K315T, N316A, or R317A. After 48 h of expression, the accumulation of polyQ$_{79}$-EGFP intracellular inclusions was visualized by fluorescence microscopy. Scale bar, 20 μm. (B) Neuro2A cells were transiently co-transfected with expression vectors for polyQ$_{79}$-EGFP together with empty vector (control), UPRplus WT, or the mutants K122L, N316A, R317A, or K315T. After 48 h, high molecular weight (HMW) polyQ$_{79}$-EGFP species were measured in cell extracts prepared in Triton X100 using western blot with an anti-GFP antibody (upper panel). Bottom panel: Levels of Hsp90 were monitored as a loading control.

Figure S4. Analysis of the promoter regions of genes regulated by UPRplus. (A) The motif pattern analysis in the promoter region showing that the canonical ERSE I and ERSE II are present in the promoters of the five top genes upregulated by UPRplus. The promoter sequences spanning 15 kb upstream and 2 kb downstream of the transcriptional start site (TSS) were examined. The consensus sequence is shown in the

indicated boxes. The blue box is the consensus sequence to which NF-Y binds and the red box is the consensus sequence to which ATF6 binds. (B) Frequency of transcription factor binding motifs (TFBMs) of transcription factors XBP1s and ATF6f at 10,000 bp upstream of the transcription start site. (C) Representation of the promoter region 10,000 bp upstream of the TSS for the five UPRplus upregulated genes in the positive and negative strands. Vertical marks correspond to the presence of specific motifs for XBP1s in red and ATF6f in blue. (D) Graphical representation of a nucleic acid multiple sequence alignment of motifs as sequence logo to ATF6f, XBP1s, and both ATF6f/XBP1s, indicating the relative frequency of each nucleic acid in the motif.

Figure S5. Validation of the knockdown experiments for UPRplus-regulated genes. (A) HEK293T cells were transiently transfected with siRNA against indicated genes or scrambled siRNA (siSCR) as control. After 48 h, the expression levels of the indicated mRNAs were measured by real-time RT-PCR. All samples were normalized to β-actin levels. mRNA levels are expressed as fold increase over the value obtained in the control condition (siSCR). (B) After 48 h, the EGFP expression levels were measured by real-time PCR to control transfection efficiency. All samples were normalized to β-actin levels. mRNA levels are expressed as fold increase over the value obtained in the control condition (siSCR). In all experiments the mean and standard error is presented of three independent experiments. Statistical analysis was performed using Dunnett's multiple comparisons test (**: $p < 0.01$; ***: $p < 0.001$).

Figure S6. Validation of UPRplus expression in neurons. (A) Neuro2A cells were transiently co-transfected with expression vectors for polyQ$_{79}$-EGFP and XBP1s, ATF6f, UPRplus, or empty vector (Control). After 24 h, expression levels of human ATF6f and XBP1s were measured by real-time RT-PCR. All samples were normalized to β-actin levels. (B) Validation of UPRplus, XBP1s, or ATF6f expression in primary cortical neurons. Primary cortical neurons were infected at 1 day in vitro (DIV) with adeno-associated virus (AAV) encoding for UPRplus, XBP1s, ATF6f, or empty vector (control). After 6 DIV, expression levels of human ATF6f and XBP1s were measured by real-time RT-PCR. All samples were normalized to β-actin levels. (C) Validation of UPRplus, XBP1s, or ATF6f expression in YAC128 mice injected. Three-months old YAC128 mice were injected into the striatum with AAV-UPRplus, AAV-ATF6f, AAV-XBP1s, or AAV-Mock vector (control) using unilateral stereotaxis surgery. Four weeks later, the striatum was dissected and human XBP1s and ATF6f levels analyzed by PCR in each group.

Figure S7. Effects of UPRplus expression on the survival of dopaminergic neurons after exposure to 6-OHDA. (A) Analysis of the percentage of recovery in the cylinder test performance of animals treated with AAV-UPRplus. (B-C) Histograms show the number of TH-positive neurons of injected and non-injected sides in 25 µm midbrain serial sections separated by 100 µm and covering the entire SNpc. The number of serial sections indicates the orientation from anterior to posterior from animals injected with AAV-Mock (B) or AAV-UPRplus (C). Data represent the mean and standard error from 8 animals per group Statistical analysis was performed using Dunnett's multiple comparisons test. *: $p < 0.05$, **: $p < 0.01$.

Figure S8. Determination of safety and stability of UPRplus expression in the brain. (A) The expression of TH was performed by immunohistochemistry in midbrain sections from mice injected with AAV-UPRplus, AAV-ATF6f, AAV-XBP1s, or AAV-Mock for 1 year. The total content of TH-positive somas was measured in midbrain sections covering the entire SNpc, in the non-injected (control) and injected side, for each group. Data represent the mean and standard error from 4 animals per group. (B) The expression of UPRplus was monitored in the brain obtained from AAV-UPRplus, AAV-XBP1s-HA, AAV-ATF6f-HA or AAV-Mock injected animals for 1 year using immunohistochemistry with an anti-HA antibody. (Scale bar: 1 mm, upper panel and 100 µm, bottom panel).

Figure S9. Characterization of α-synuclein preformed fibrils. (A) Frequency distribution of α-synuclein preformed fibrils (PFFs) length by transmission electron microscopy. Histogram of distribution for relative abundance of post-sonicated fibrils. 600 structures were counted. (B) Primary cortical neurons were treated with PBS (Control) (left panel) or with α-synuclein PFF (1 ng) at 7 day in vitro (DIV) (middle panel). After 7 DIV the phosphorylated form of α-synuclein (p-α-syn) (green), microtubule associate protein 2 (MAP2) (red) and nuclear staining with DAPI (blue) were detected by immunofluorescence. Higher magnification of middle panel (right panel). Scale bar: 50 µm (left and middle panel), 20 µm (right panel).

Figure S10. Analysis of mHtt levels in a viral HD model. (A-B) Three-month-old wild type mice were co-injected into the striatum by stereotaxis with a mixture of AAVs encoding a mHtt construct (Htt588^{Q95}-mRFP) together with AAV-UPRplus, AAV-XBP1s, AAV-ATF6f, or AAV-Mock (control). Animals were then euthanized 2 weeks post-injection and brain striatum tissue was dissected for western blot analysis using an anti-polyQ antibody. β-actin levels were monitored as a loading control (bottom panel).

Figure S11. Validation of the proteomic analysis. The mRNA levels of selected UPR-upregulated genes were monitored in HEK293T cells infected with AAV-empty (control), AAV-XBP1s or AAV-ATF6f viral particles. After 48 h the relative mRNA levels of indicated genes were measured by real-time PCR. As a positive control, cells were treated with 1 μg/ml tunicamycin for 8 h (Tm). All samples were normalized to β-*actin* levels.